

**IR Detector Technology Workshop
Feb. 7 - 9, 1989
NASA Ames Research Center**

GERMANIUM BLOCKED IMPURITY BAND (BIB) DETECTORS

**E. E. Haller^{1,2}
H. Baumann^{1,2}
J. Beeman²
W. L. Hansen²
P. N. Luke²
M. Lutz^{1,2}
C. S. Rossington^{1,2,3}
I. C. Wu^{1,2}**

¹University of California at Berkeley

²Lawrence Berkeley Laboratory, UCB

**³Present address: Hewlett-Packard, Opto-Electronic Division,
350 W. Trimble Rd., San Jose, CA 95131**

CONTENTS

1 . Introduction

2 . Ge BIB

3 . Ge BIB Detector Development

3.1.Epitaxial Blocking Layer Devices

3.1.1.Ge epitaxy

3.1.2.Characterization of epi layers

3.1.3.Preliminary detector test results

3.2.Ion Implanted BIB Detectors

4 . Conclusions

1 . INTRODUCTION

- **Extrinsic, photoconductive semiconductor detectors cover the infrared spectrum from a few μm up to 250 μm .**
- **Photoconductors exhibit high responsivity and low noise equivalent power.**
- **The Si blocked impurity band (BIB) detector invented by M. D. Petroff and M. G. Stapelbroek has a number of advantages over standard bulk photoconductors. These include:**
 - **smaller detection volume leading to a reduction of cosmic ray interference**
 - **extended wavelength response because of dopant wavefunction overlap**
 - **photoconductive gain of unity**

2 . Ge BIB

- **The success of Si BIB detectors has been a strong incentive for the development of Ge BIB detectors.**
- **The advantages of Si BIB detectors stated above should, in principle, be realizable for Ge BIB detectors.**
- **If Ge BIB detectors can be made to work out to 250 μm with high responsivity and sufficiently low dark current, they could replace stressed Ge:Ga photoconductors.**
- **Can the dark current be reduced to acceptable levels?**

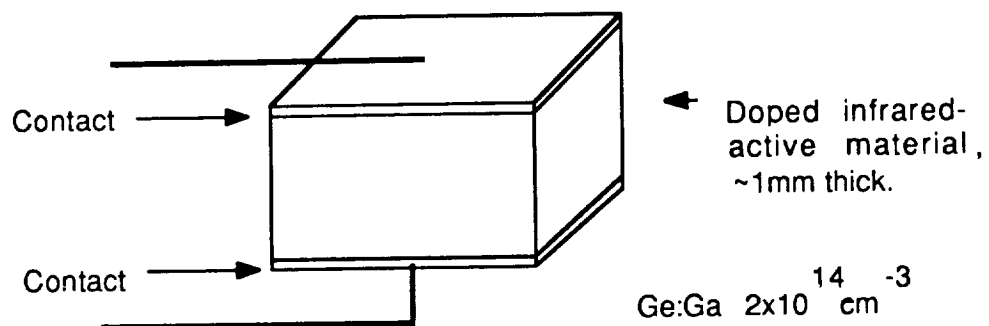


Figure 1(a). Schematic of conventional detector.

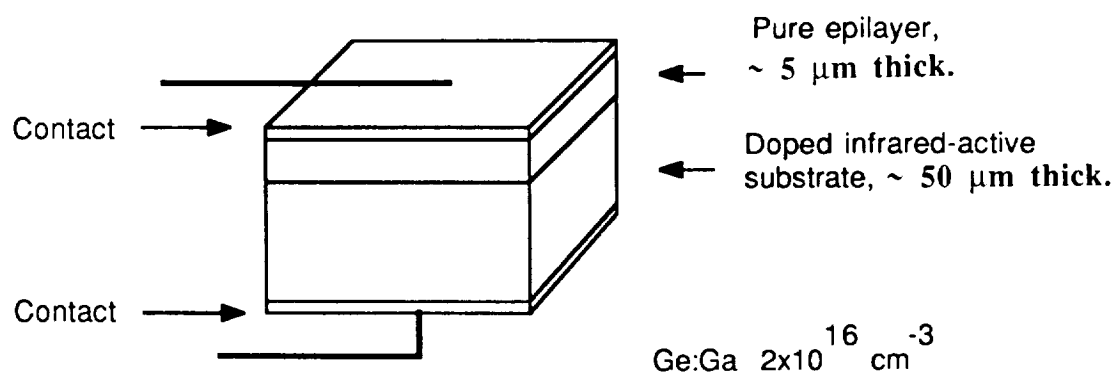


Figure 1(b). Schematic of BIB detector.

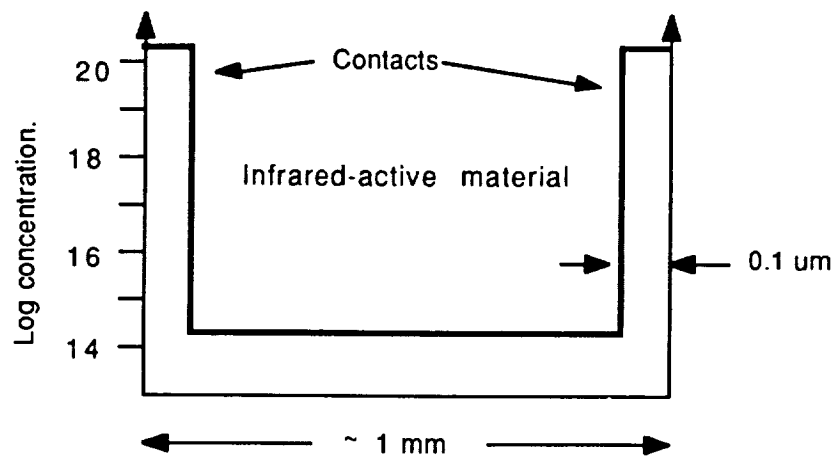


Figure 2(a). Doping levels in a conventional Ge detector.

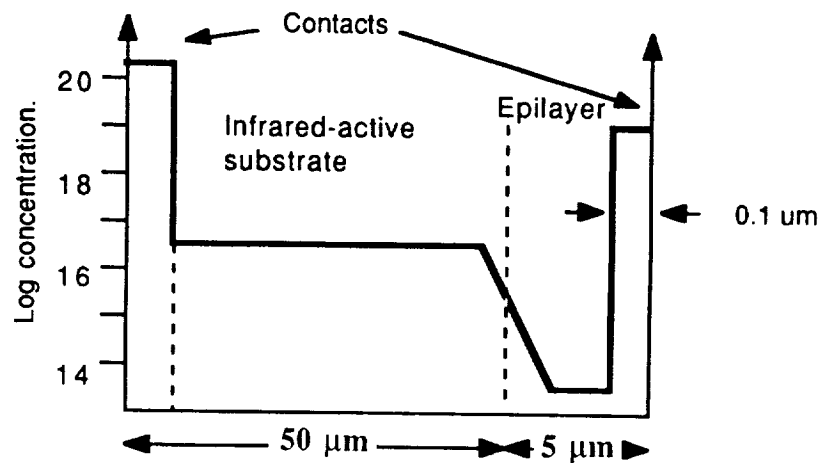


Figure 2 (b). Doping levels in a Ge BIB detector.

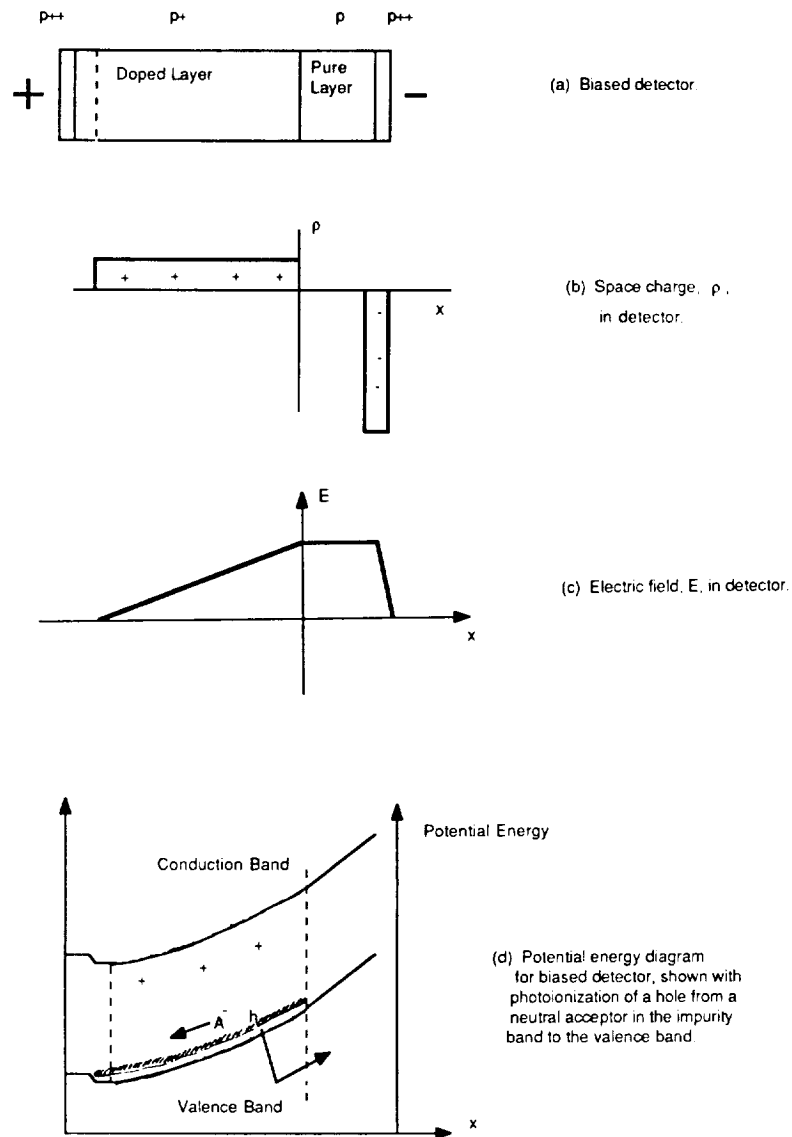


Fig. 3. Schematics of space charge, electric field and potential energy for a reverse biased p-type BIB detector.

3. Ge BIB DETECTOR DEVELOPMENT

3.1. Epitaxial Blocking Layer Devices

3.1.1. Ge epitaxy

- Whereas Si epitaxy techniques have been developed to a very high degree of perfection, Ge epitaxy has been attempted only on a few occasions.
- Ge chemistry is very different from Si chemistry.
- Ultra-pure Ge compounds [$\text{Ge}(\text{CH}_3)_4$, $\text{Ge}(\text{C}_2\text{H}_5)_4$] are being developed for III-V semiconductor technology. They may be useful to Ge epitaxy.

Substrate choice and preparation

- We have used a number of different crystals with various crystallographic orientations in the development of Ge epitaxy:
 - n-type wafers ($\sim 10^{11} \text{ cm}^{-3}$) are used for the electrical characterization of the epitaxial layers which are typically p-type because of residual copper contamination (junction isolation).
 - p-type wafers ($\sim 10^{15} \text{ cm}^{-3}$) are used for I-V comparison tests with conventional photoconductors.
 - p-type wafers ($\sim 2 \times 10^{16} \text{ cm}^{-3}$, low compensation) are used for Ge BIB detectors.

- **Wafer polishing process:**
 - **mechanical planar lapping with alumina slurry.**
 - **mechano-chemical polishing with syton containing H_2O_2 .**
 - **brief etch in $\text{HNO}_3\text{:HF}$ (3:1) followed by soak in HF (1% in H_2O) to remove oxides.**

- **Epitaxy:**
 - **first experiments with atmospheric pressure vapor phase epitaxy (VPE). Disadvantage: high substrate temperature, H_2 diluted feed gas (contamination, diffusion of dopants into the blocking layer).**
 - **current experiments are performed with low pressure VPE. Advantage: low substrate temperature.**

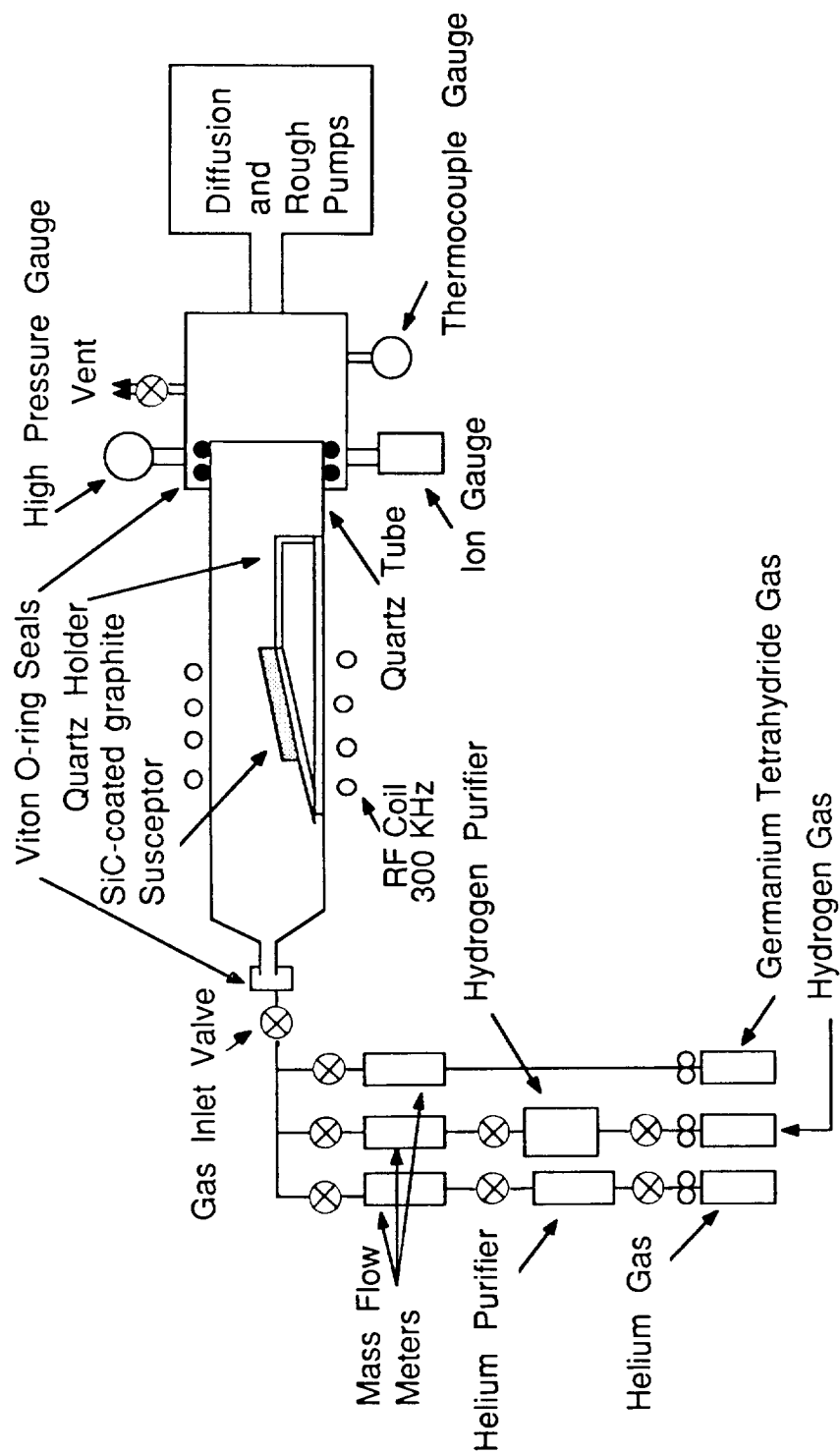


Fig. 4. Schematic of horizontal VPE apparatus. Quartz tube is 5.7 cm O.D. x 75 cm long.

3.1.2. Characterization of epi layers

- **Optical micrographs**
- **Variable temperature Hall effect and resistivity**
- **Rutherford backscattering (channeling) spectrometry (RBS)**
- **Secondary ion spectrometry (SIMS)**
- **Spreading resistance measurements**

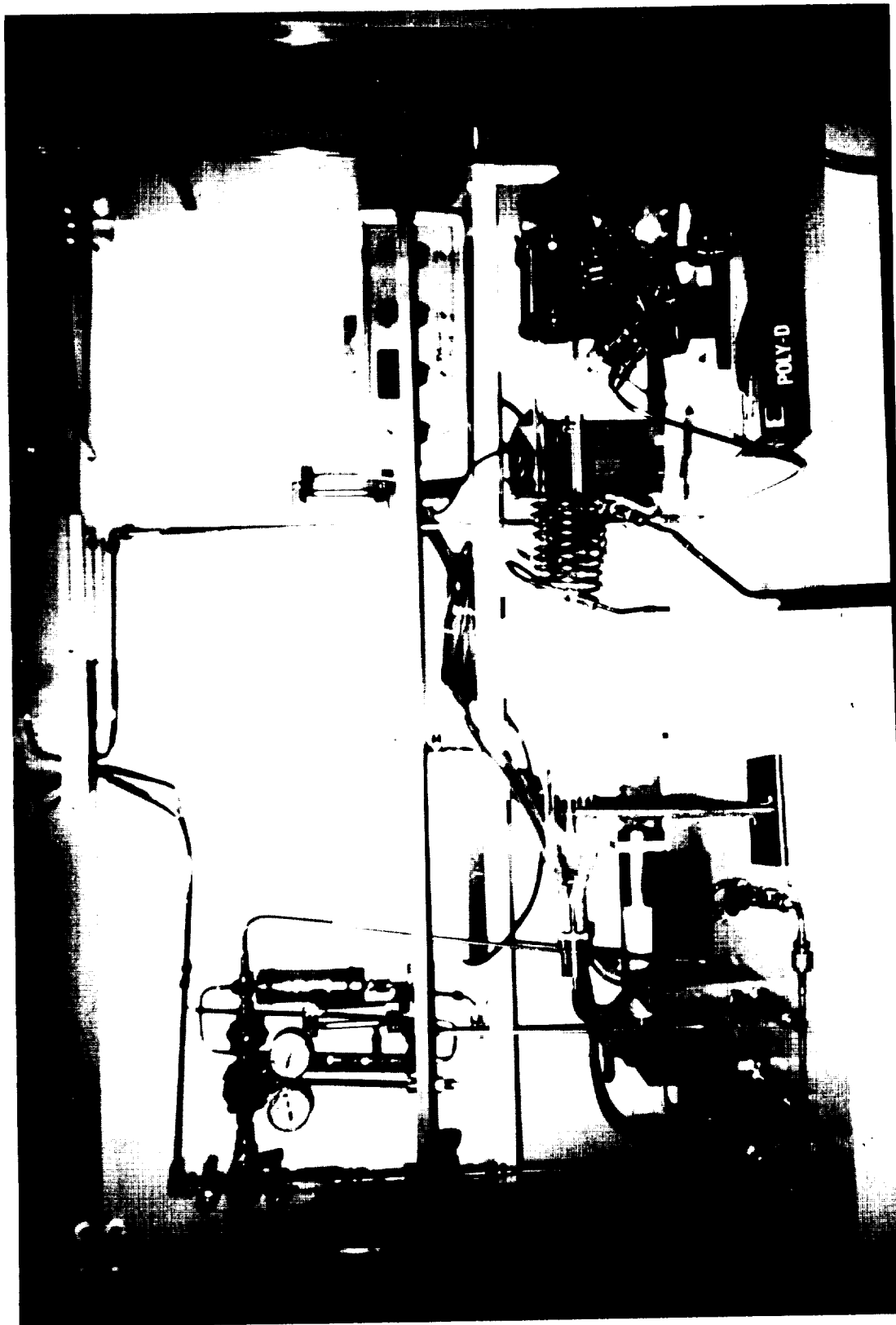
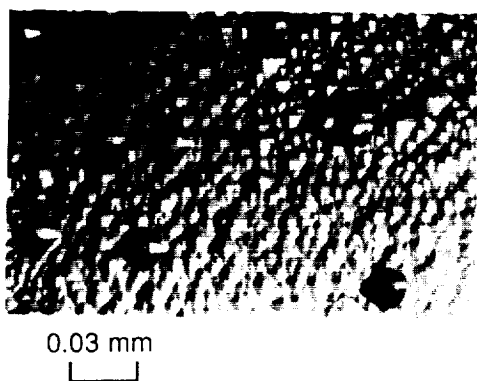
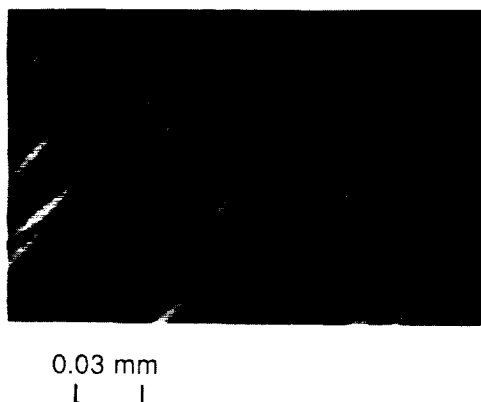


Fig. 5. Photograph of the horizontal VPE chamber.

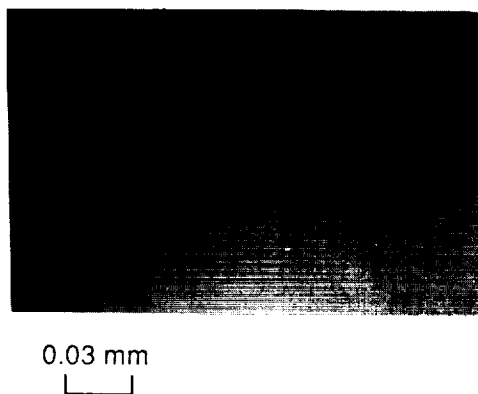
ORIGINAL PAGE
BLACK AND WHITE PHOTOGRAPH



(100) $N_D - N_A = 1 \times 10^{14} / \text{cm}^3$
580 °C; 5 sccm GeH_4 ,
with H_2 reduction step,
polycrystalline deposition



(113) $N_D - N_A = 2 \times 10^{14} / \text{cm}^3$
580 °C; 5 sccm GeH_4 ,
with H_2 reduction step,
no growth (etching)



(113) $N_D - N_A = 5 \times 10^{11} / \text{cm}^3$
550 °C; 10 sccm GeH_4 ,
no H_2 reduction step,
single crystal deposition

Fig. 6. Optical micrographs of Ge epi layers.

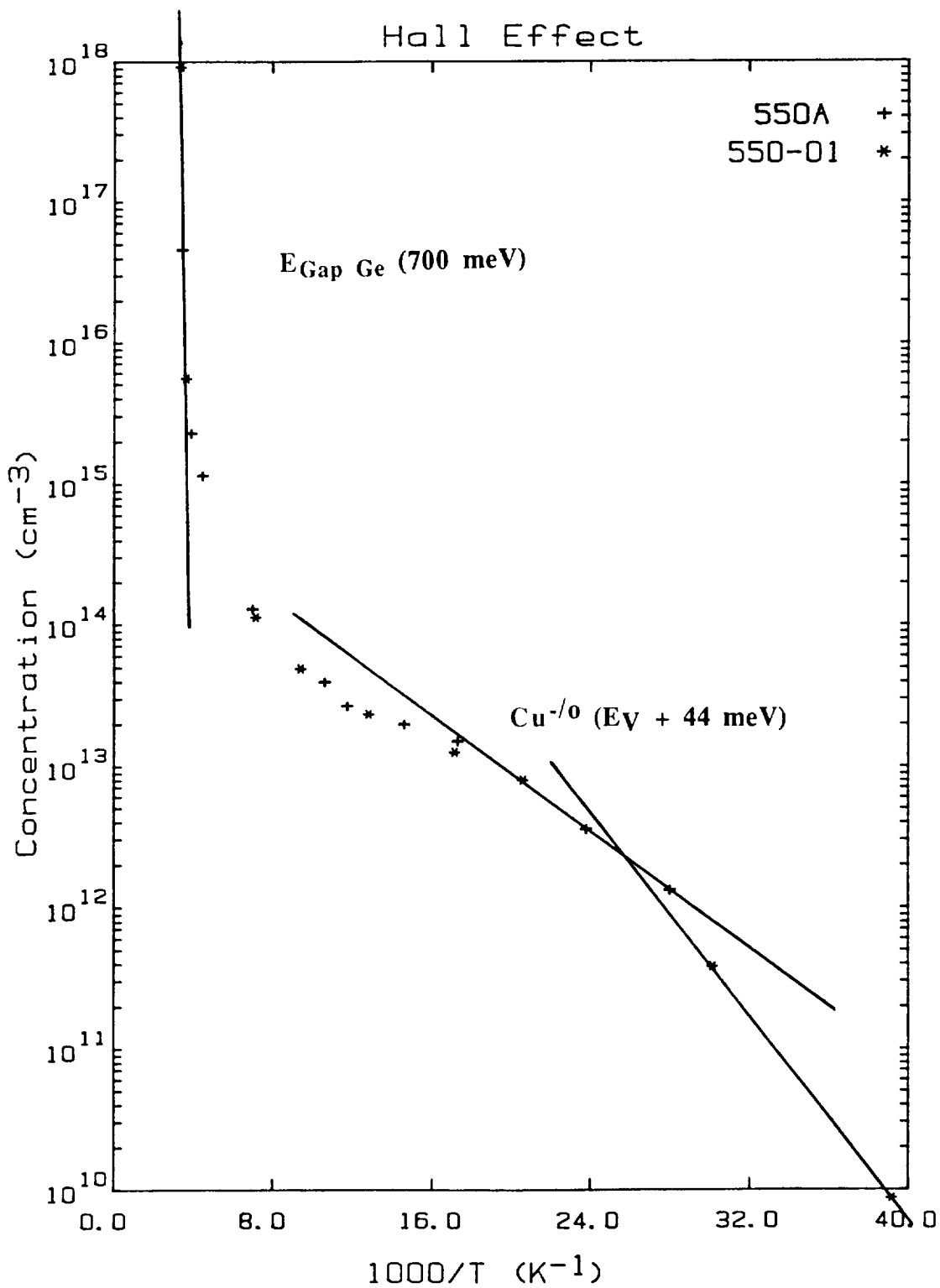


Fig. 7. Variable temperature Hall effect measurements of a Ge epilayer on an n-type [113] substrate. The hole freeze-out curves indicate a light copper contamination. The two curves (+, *) are measurements of the same sample and demonstrate reproducibility.

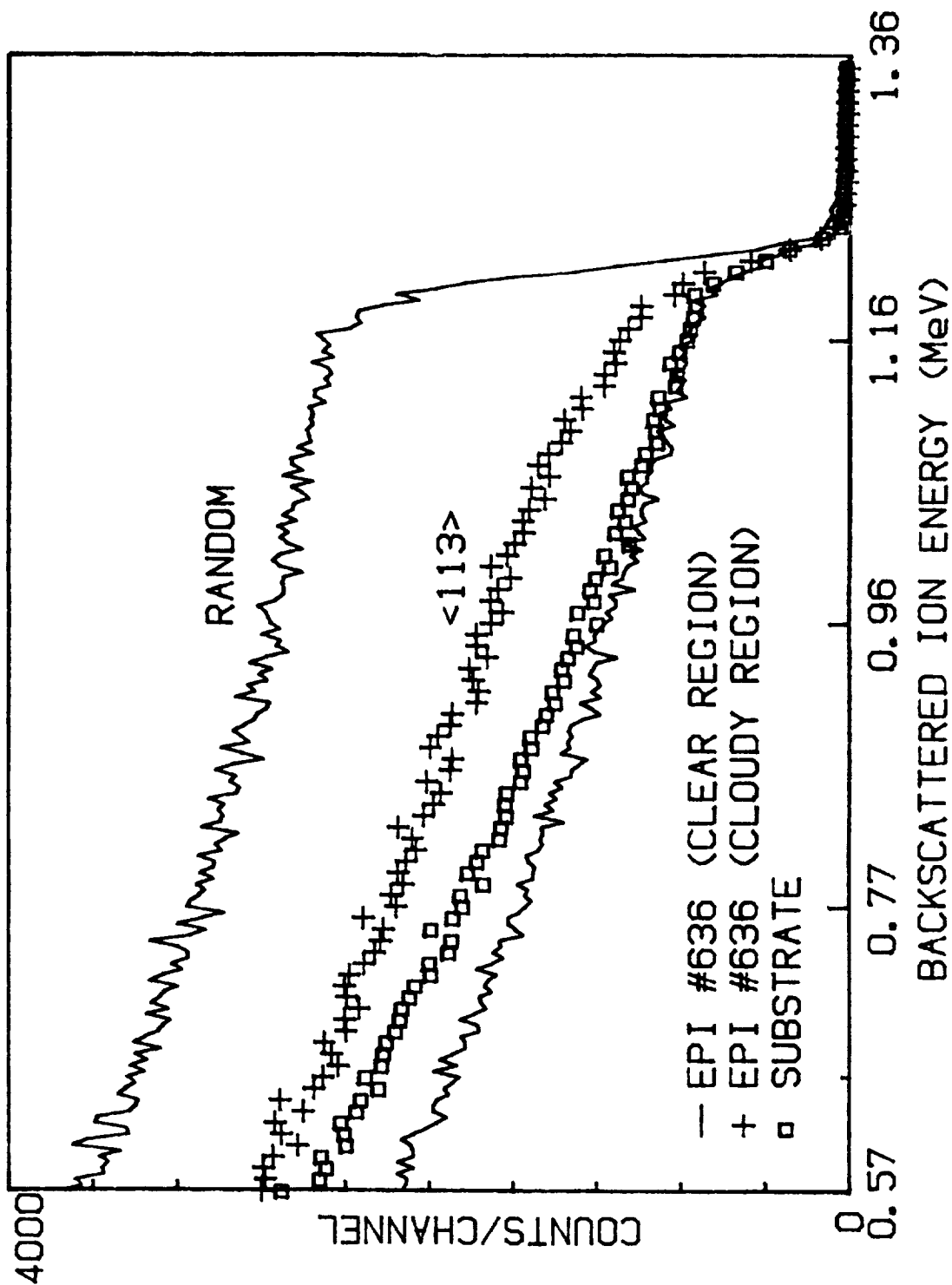


Fig. 8. RBS channeling spectra of a Ge epi film (#636). The "cloudy" region shows significant dechanneling indicating a high defect concentration.

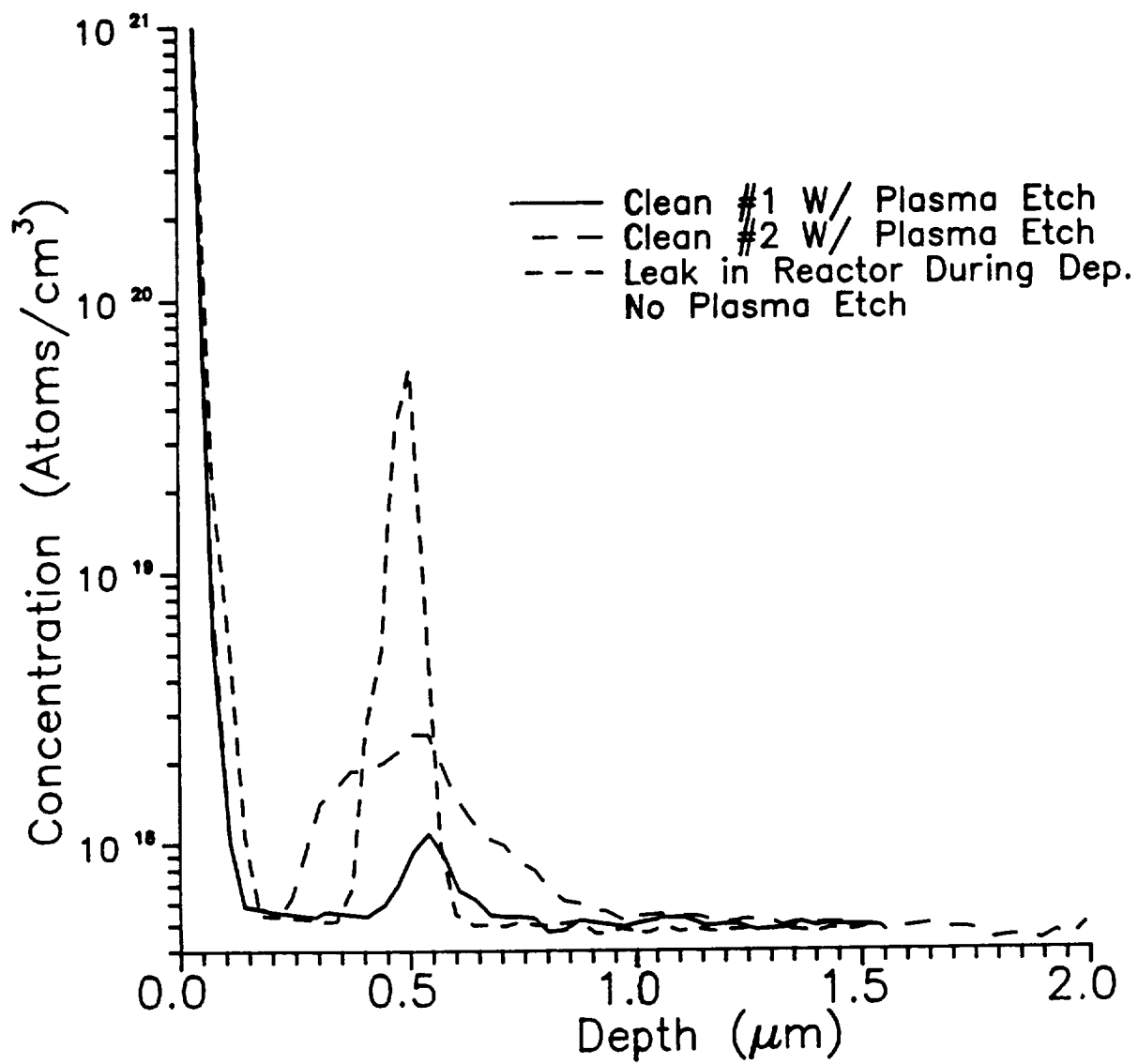


Fig. 9. SIMS of LPVPE Epi Films:
Oxygen Concentration

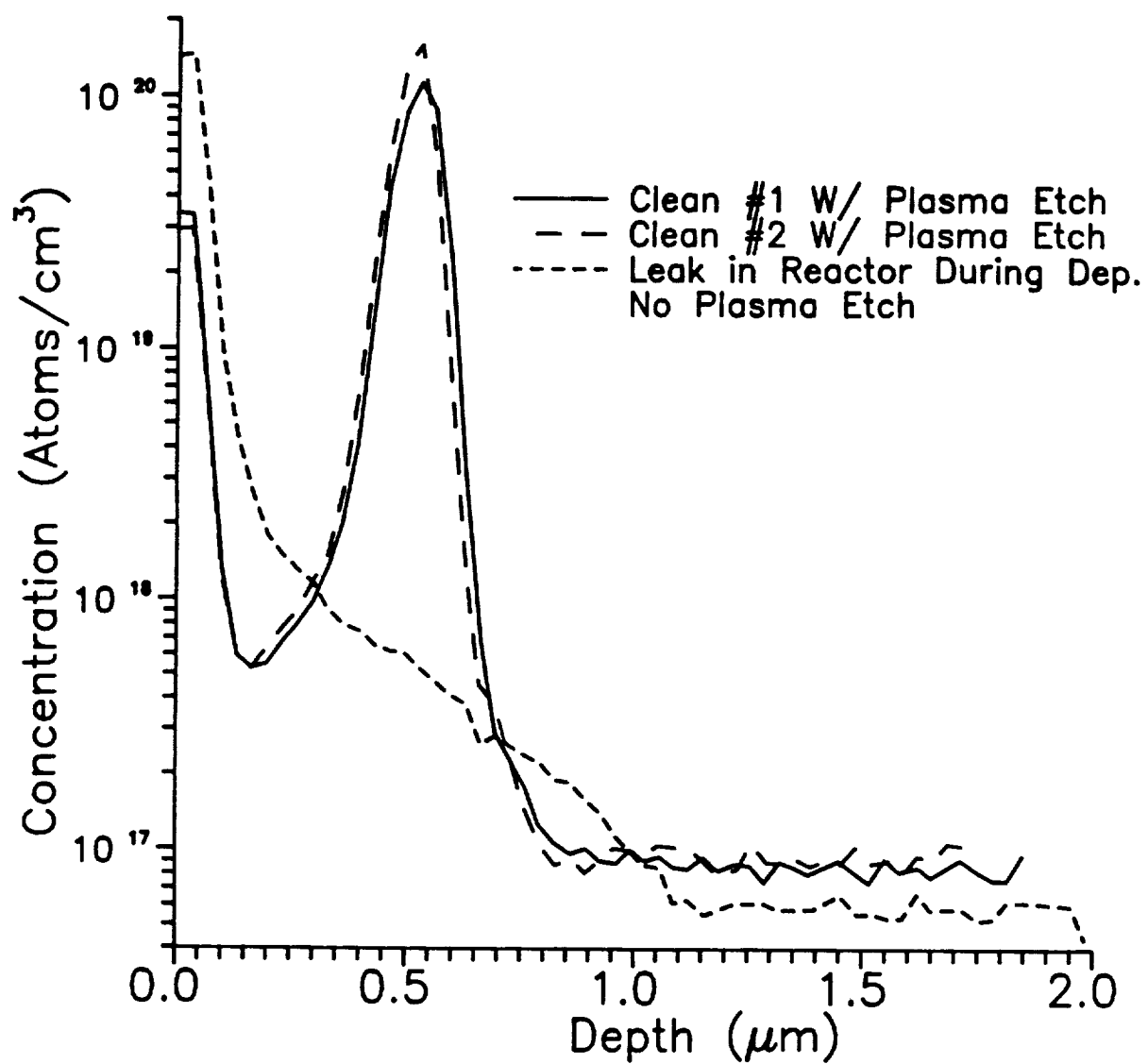


Fig. 10. SIMS of LPVPE Epi Films:
Carbon Concentration

3.1.3. Preliminary detector test results

- **Responsivity**
- **Dark current**

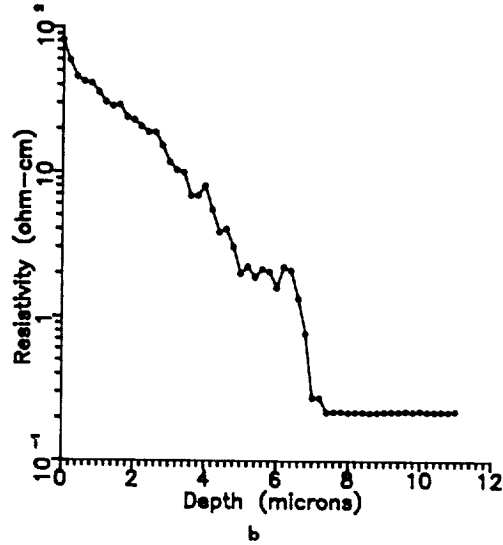
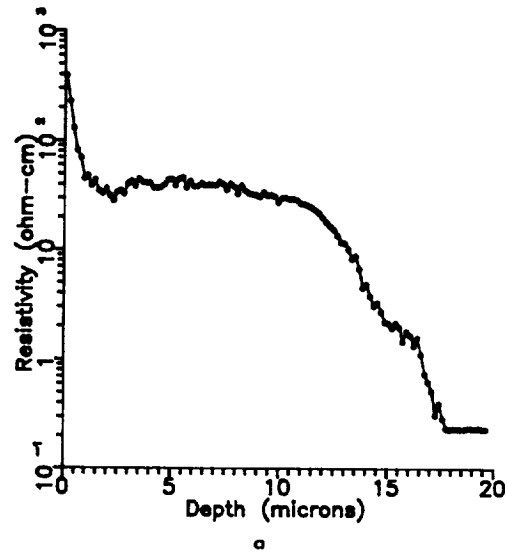


Fig. 11. Spreading resistance as a function of depth from the epilayer surface for: (a) an area of epilayer close to the leading edge of the wafer in II-16 where the growth rate was $\sim 0.06 \mu\text{min}^{-1}$, and (b) an area of epilayer farthest from the leading edge of the same wafer where the growth rate was $\sim 0.02 \mu\text{min}^{-1}$. The slight rise in resistivity at the very surface is due to the native oxide.

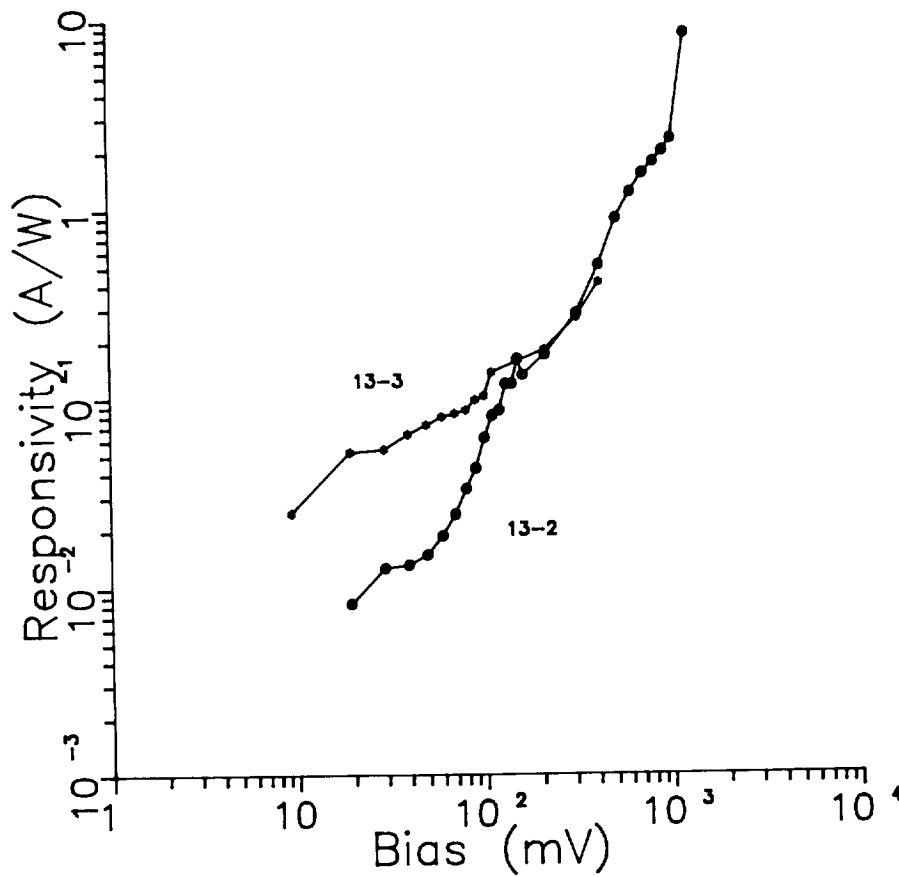


Fig. 12. Responsivity as a function of bias for detectors 13-2 and 13-3 at 2.3 K under reverse bias. The substrate material is moderately doped ($5 \times 10^{15} \text{ cm}^{-3}$). Such material exhibits hopping conduction but does not have extended wavelength spectral response. Tests were performed with a narrow band filter at $\lambda = 98.9 \text{ } \mu\text{m}$.

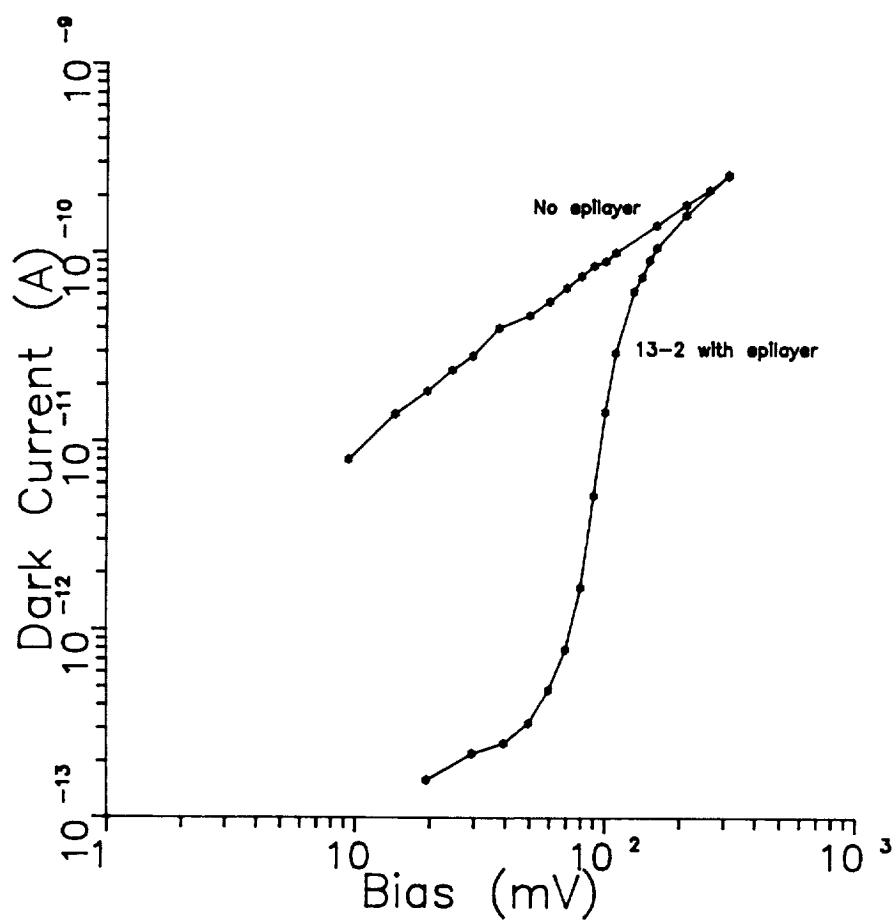


Fig. 13. Dark current as a function of detector bias for detector 13-2 with an epilayer and for the same "detector" without an epilayer at 2.3 K under reverse bias. Below a bias of ~ 100 mV, the blocking layer effectively reduces hopping conduction in this moderately doped material ($N_A - N_D = 5 \times 10^{15} \text{ cm}^{-3}$).

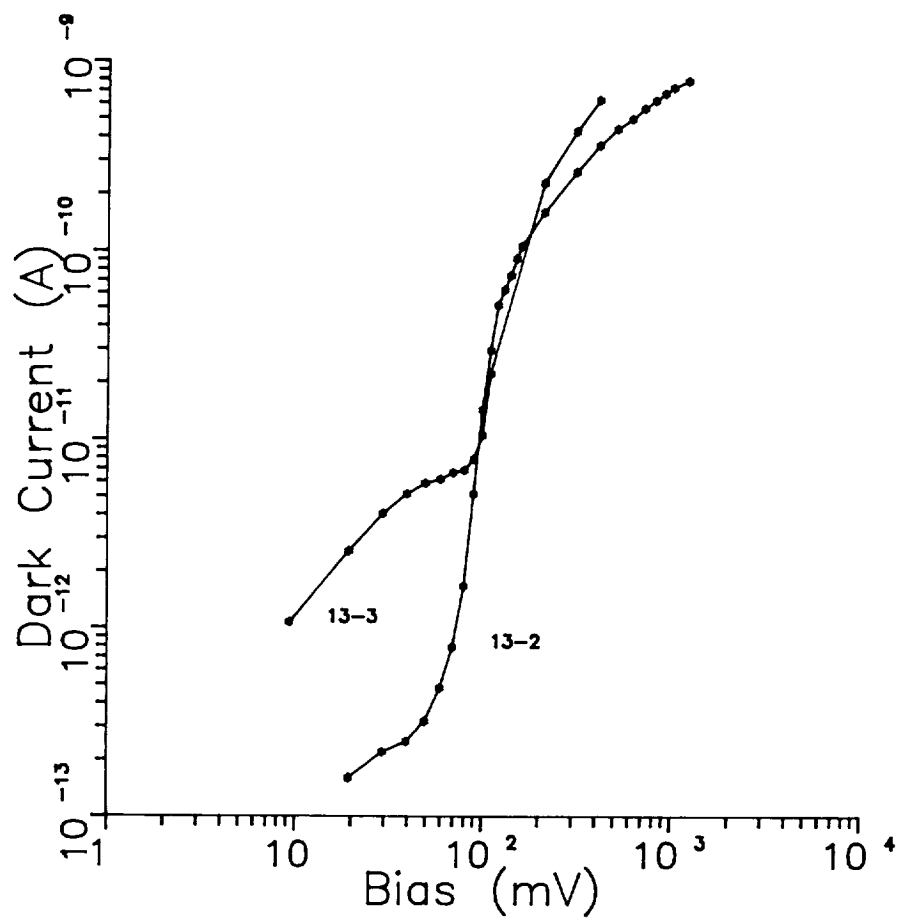


Fig. 14. Dark current as a function of bias for detectors 13-2 and 13-3 at 2.3 K under reverse bias.

3.2. Ion Implanted BIB Detectors

- **Concept:**
 - In case pure and structurally perfect epitaxial layers are hard to produce, we can resort to implantation of dopants into an ultra-pure crystal.
- **Low energy B⁺-implantation tests:**
 - three B⁺ energies: 150 keV, 95 keV, 50 keV form a 0.4 μm thick layer with $N_A = 3.5 \times 10^{16} \text{ cm}^{-3}$.
 - annealing at 400°C for one hour in argon.
 - extended wavelength response.
 - responsivity = 0.5 A/W, dark current $< 10^{-14} \text{ A}$, at bias = 100 mV and $T = 2.0 \text{ K}$. NEP $\approx 4 \times 10^{-16} \text{ W}/\sqrt{\text{Hz}}$.

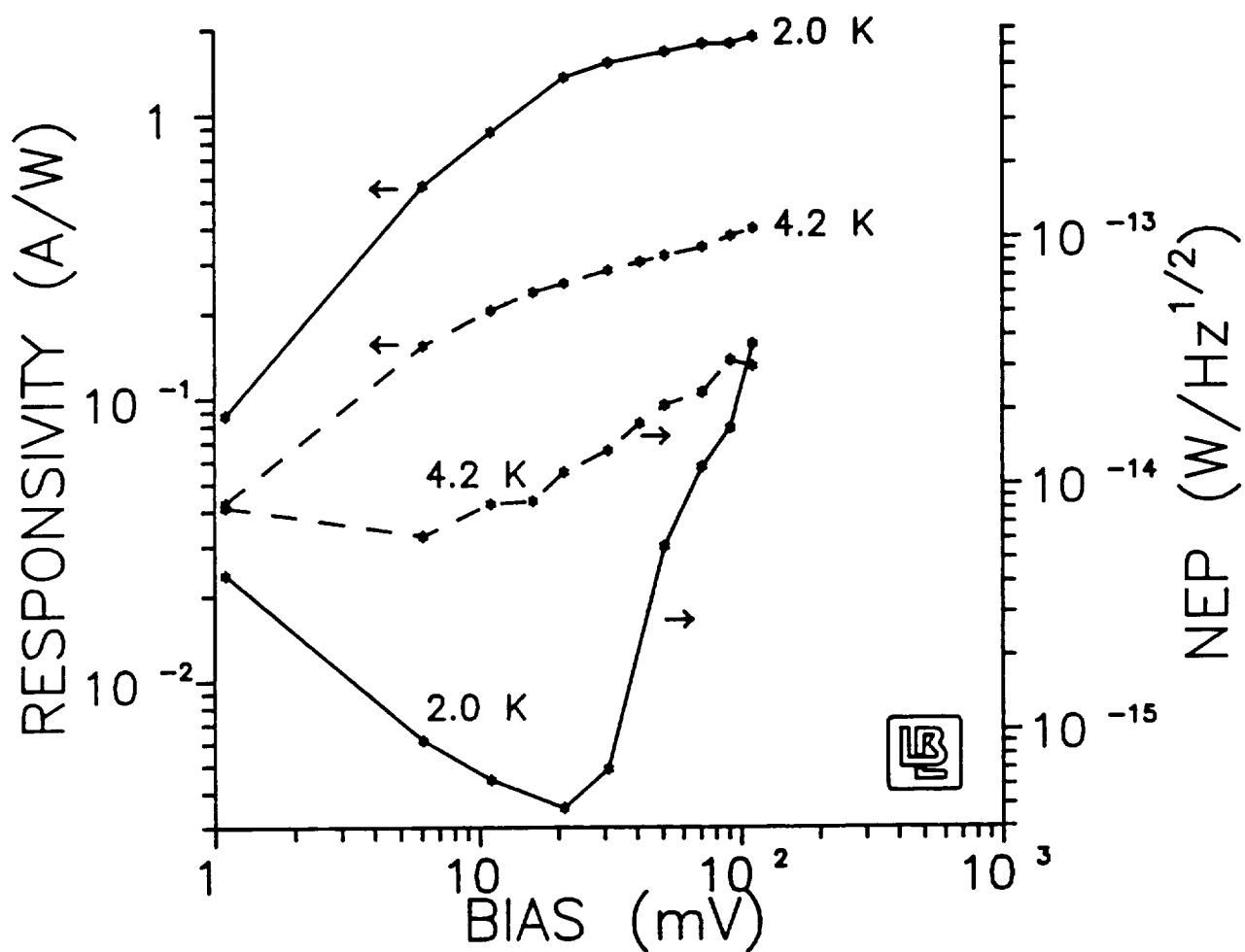


Fig. 15. Responsivity of a Ge BIB detector, low energy B⁺-implant type. Active layer depth = 0.6 μm , $[B] = 1 \times 10^{16} \text{ cm}^{-3}$, $\lambda_{\text{filter}} = 98.9 \mu\text{m}$, $f_{\text{chopper}} = 23 \text{ Hz}$

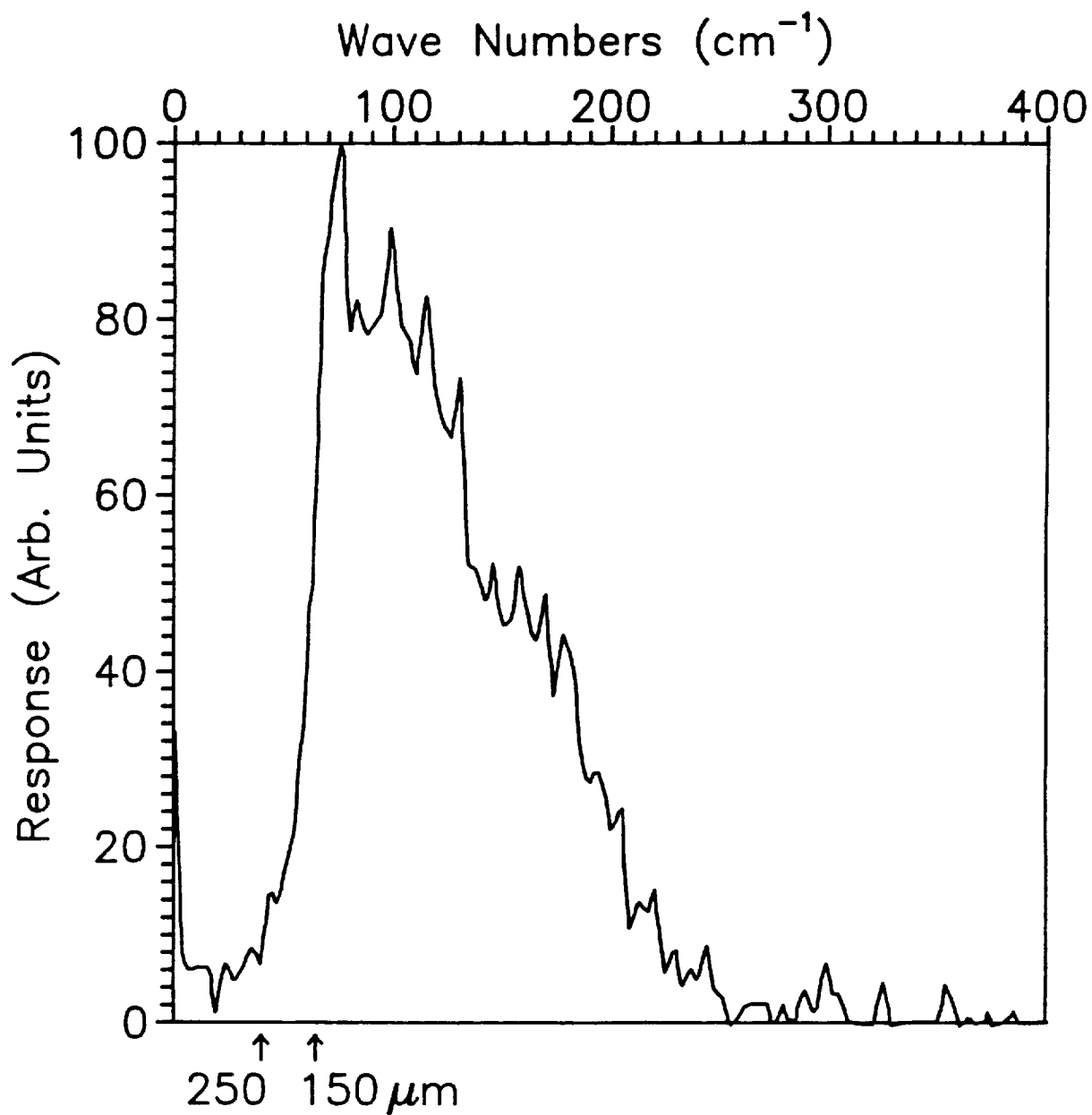


Fig. 16. Spectral response of Ge BIB detector, low energy B⁺-implantation type.

- **High energy B⁺-implantation tests:**
 - **14 implant energies up to 4 MeV doubly charged boron ions lead to a 5 μm thick layer with N_A = 1 x 10¹⁶ cm⁻³.**
 - **Variable temperature Hall effect and resistivity measurements indicate full activation of shallow acceptor dopant B. No deep levels are detectable after annealing. Below 15 K, hopping conduction becomes dominant.**
 - **Infrared transmission measurements and device tests are in progress.**

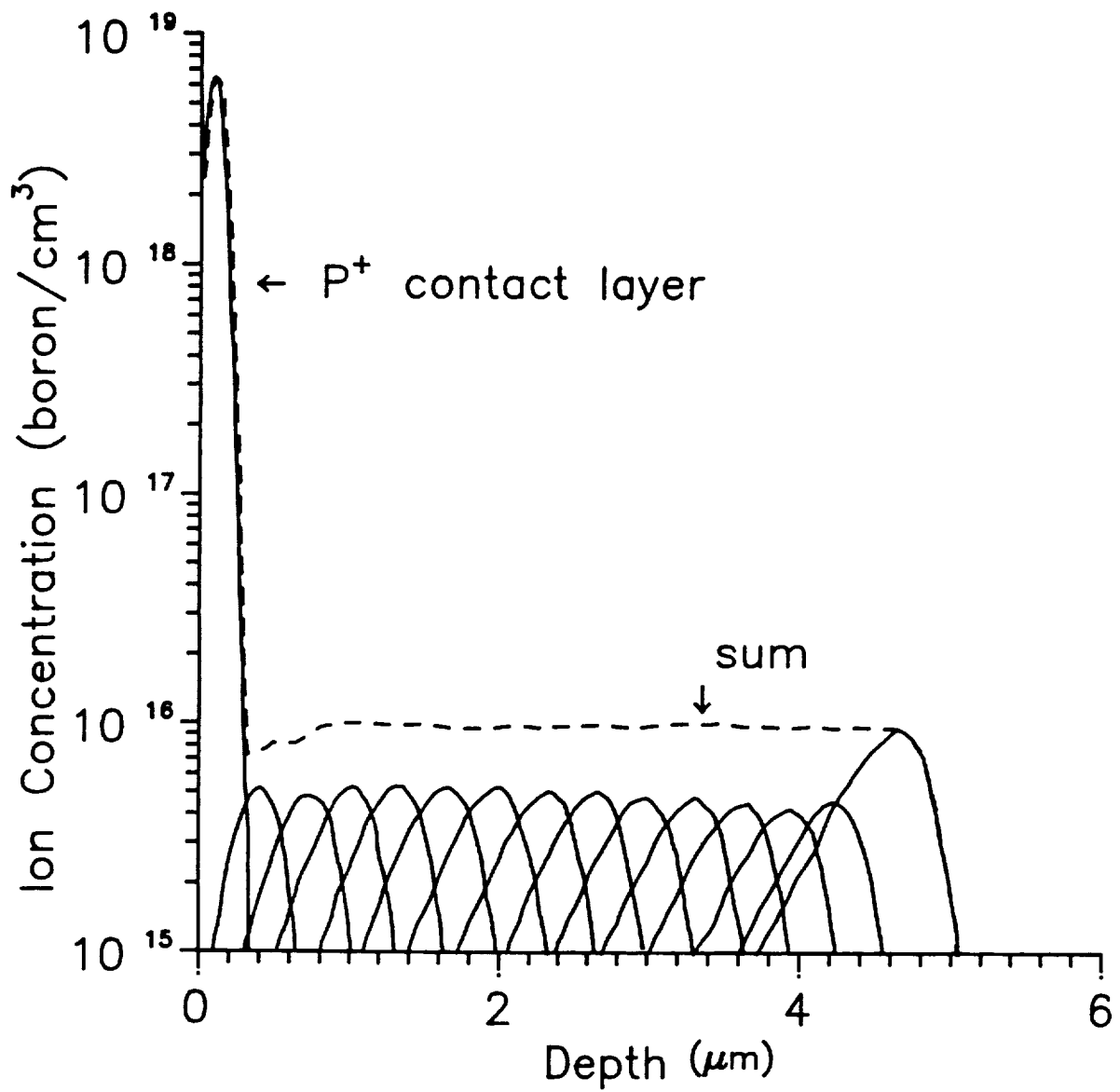


Fig. 17. Ge BIB, high energy ion implant profile

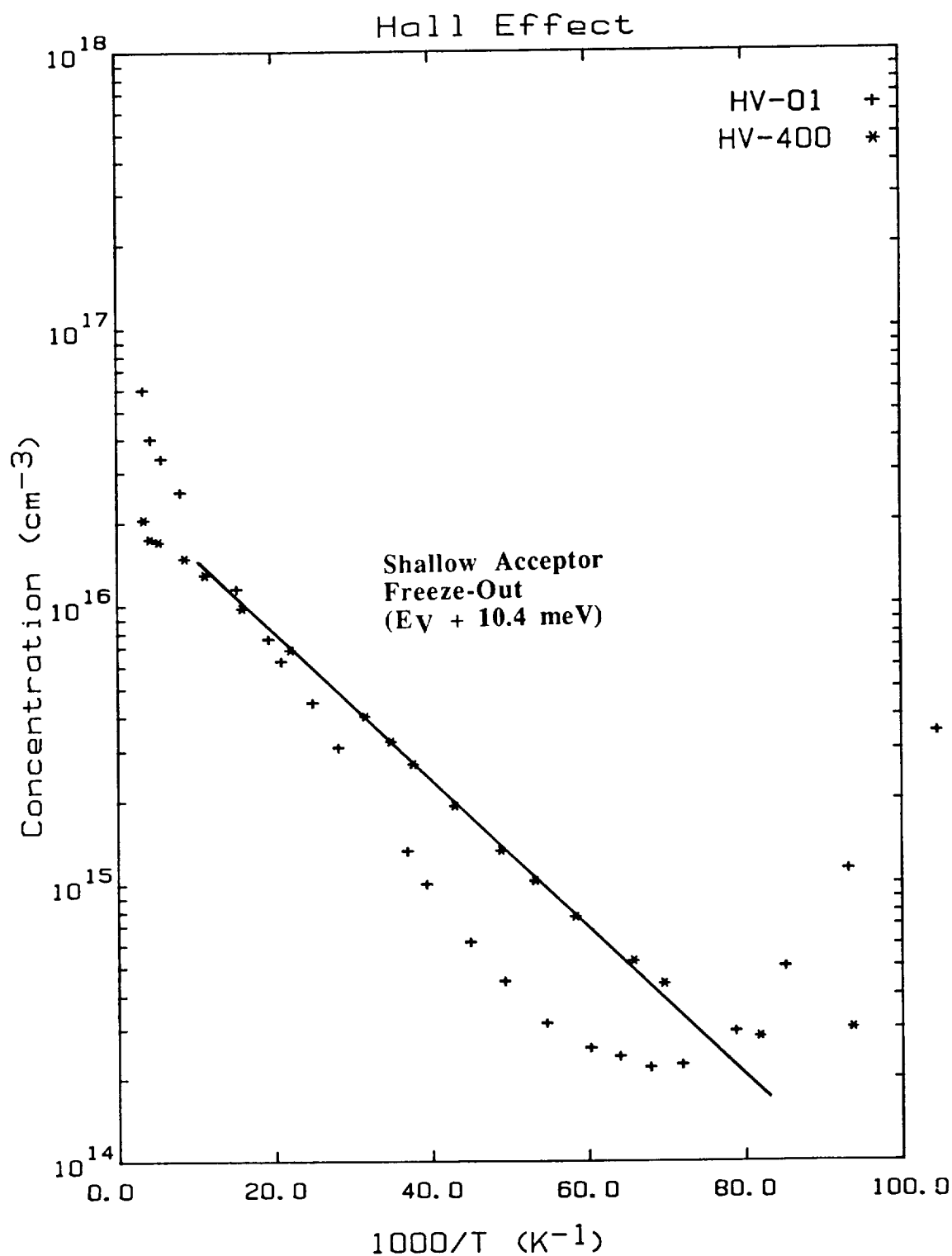


Fig. 18. Free carrier freeze-out of high energy B^+ -implanted layer. Before annealing (+), the slope of the freeze-out curve is steeper than after annealing (*). The latter slope corresponds to $\sim 10.4 \text{ meV}$, the binding energy of shallow boron acceptors. Below 15 K, hopping conduction becomes dominant.

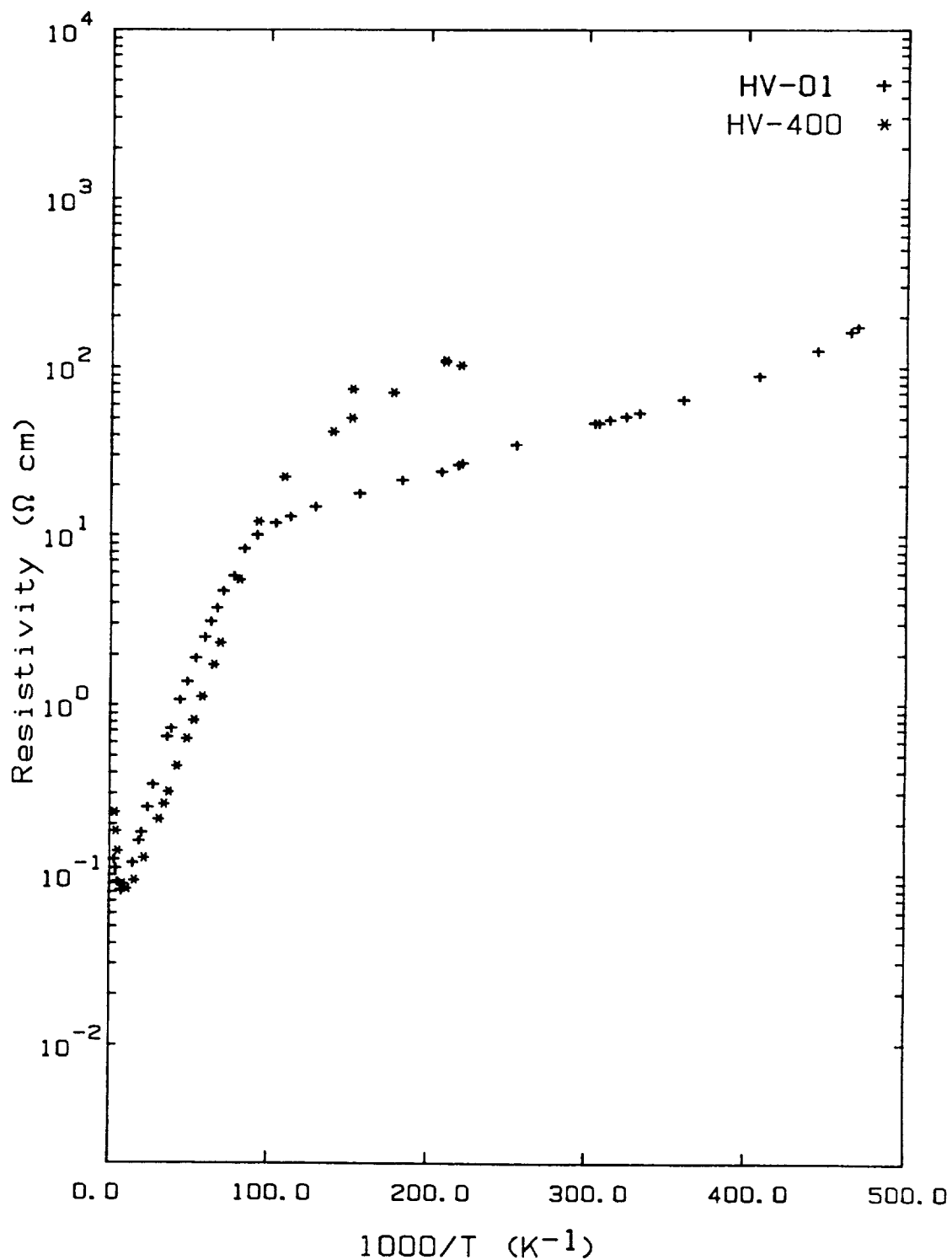


Fig. 19. Resistivity as a function of inverse temperature of the high energy B⁺-implant layer before (+) and after (*) annealing. Hopping conduction becomes dominant below 15 K.

4. CONCLUSIONS

- **A LPVPE technique for the low temperature growth of epitaxial Ge layers has been developed.**
- **Hall effect and resistivity measurements indicate that the epi layers are lightly p-type due to residual copper contamination.**
- **First generation Ge BIB detectors made with moderately doped substrates ($5 \times 10^{15} \text{ cm}^{-3}$) exhibit effective blocking of the hopping current.**
- **First generation Ge BIB detectors exhibit responsivities around 1 A/W.**
- **Second generation devices using low pressure VPE are being processed.**
- **Ion implanted active layers are tested.**
- **It is currently not known what temperatures will be required to reduce the dark current down to levels which are acceptable for SIRTf applications.**

